

## Influence of Microcapsule Shell Material on the Mechanical Behavior of Epoxy Composites for Self-Healing Applications

Manorama Tripathi,<sup>1,2</sup> Rahamtullah,<sup>2</sup> D. Kumar,<sup>2</sup> Chitra Rajagopal,<sup>1</sup> Prasun Kumar Roy<sup>1</sup>

<sup>1</sup>Centre for Fire, Explosive and Environment Safety, DRDO, Timarpur, Delhi 110054, India

<sup>2</sup>Department of Applied Chemistry and Polymer Technology, Delhi Technological University, Delhi 110042, India

Correspondence to: P. Kumar Roy (E-mail: pk\_roy2000@yahoo.com, pkroy@cfees.drdo.in)

**ABSTRACT:** In this article, we have studied the effect of microcapsule shell material on the mechanical behavior of self-healing epoxy composites. Liquid epoxy healant was encapsulated in melamine-formaldehyde (MF) and urea-formaldehyde (UF), using emulsion polymerization technique to prepare microcapsules of different shell walls. The core content of the microcapsules, as determined by solvent extraction technique was found to be  $65 \pm 4\%$ , irrespective of the shell wall of microcapsule. Morphological investigations reveal a rough texture of the spherical microcapsules, which was attributed to the presence of protruding polymer nanoparticles on the surface. Epoxy composites containing UF and MF microcapsules (3–15% w/w) were prepared by room temperature curing and their mechanical behaviour was studied under both quasi-static and dynamic loadings. The tensile strength, modulus, and impact resistance of the matrix was found to decrease with increasing amount of microcapsule in the formulation, irrespective of the shell wall material used for encapsulation. Interestingly, substantial improvement in the fracture toughness of the base resin was observed. Morphological investigations on the cracked surface revealed features like crack pinning, crack bowing, microcracking and crack path deflection, which were used to explain the toughened nature of microcapsule containing epoxy composites. Our studies clearly indicate that the microcapsule shell wall material does not play any significant role in defining the mechanical properties of the composites. In addition, presence of secondary amine functionalities in UF and MF shell wall do not interfere with the reaction of epoxy with triethylene tetramine hardener during the curing process. © 2014 Wiley Periodicals, Inc. *J. Appl. Polym. Sci.* **2014**, *131*, 40572.

**KEYWORDS:** composites; morphology; structure-property relations

Received 17 October 2013; accepted 8 February 2014

DOI: 10.1002/app.40572

### INTRODUCTION

The last few years have seen major advances in the field of smart polymeric materials, which respond autonomically to a specific stimulus, due to their “in situ” functionality.<sup>1,2</sup> Self-healing polymers belong to a sub-category of such smart materials, where the primary objective is complete repair of minor damage in the absence of any manual intervention. In this case, the propagating crack acts as the mechanical triggering stimulus, and the response is the process of autonomic repair of the resultant damage.<sup>2</sup>

While several general self-healing strategies have been investigated, one of the most successful and versatile approach utilizes the introduction of fragile microcapsules filled with a liquid healing agent,<sup>3–7</sup> within the polymeric matrix. When the propagating crack ruptures the embedded microcapsules, the healing agent is slowly released into the crack plane through capillary action, which undergoes polymerization to reestablish the structural integrity across the crack plane. Depending on the type of

healing agent employed, it may undergo polymerization by ring opening reaction (ROP), e.g., ROP of dicyclopentadiene (DCPD) with organometallic catalyst<sup>8</sup> or alternatively, the healing agent may be chosen to undergo curing reaction with the chemical agents encapsulated separately.

Different containment structures have been explored for encapsulating liquid healing agents, and presently, urea-formaldehyde (UF) and melamine-formaldehyde (MF) are most commonly used in view of their reasonable cost, adequate strength and long shelf-life. Studies on the mechanical behavior of isolated liquid filled microcapsules have highlighted significant differences in the mechanical behavior between UF and MF microcapsules,<sup>9,10</sup> however, both exhibit a clear bursting phenomenon upon compression, with the extent of deformation being much lesser in the UF based microcapsules.<sup>11</sup>

Due to the fragile nature of microcapsules, their inclusion into the polymeric resin results in substantial deterioration in the

Additional Supporting Information may be found in the online version of this article.

© 2014 Wiley Periodicals, Inc.

**Table I.** Sample Designation and Compositional Details

Sample designation	Amount (g)		
	Epoxy resin	Hardener	Microcapsule
EP	100	13	–
EP3Z	100	13	3.4
EP5Z	100	13	5.6
EP10Z	100	13	11.3
EP15Z	100	13	16.9

Z denotes the type of microcapsule (UF: Urea-formaldehyde, MF: Melamine-formaldehyde).

mechanical properties.<sup>12</sup> However, to the best of our knowledge, no systematic empirical investigations have been performed to quantify the effect of microcapsule shell wall material on the mechanical behaviour of self-healing compositions. Majority of literature in this area deal primarily with improving the repairing efficiency,<sup>13</sup> but studies on the effect of microcapsule introduction on other mechanical properties under quasi-static and dynamic mode are rather scarce. We hypothesise that although in isolation, microcapsules of different shell wall respond to mechanical loads differently,<sup>11</sup> but in view of their fragile nature, the role of the polymer used for containment of the healing agent is immaterial.

In this article, we have quantified the effect of commonly used microcapsules on the quasi-static and dynamic properties of a representative cycloaliphatic epoxy resin. Healant encapsulated microcapsules with different shell walls (UF and MF) were prepared by emulsion polymerization technique, and dispersed within the epoxy matrix to prepare self-healing formulations. The effect of introduction of these microcapsules on the mechanical properties of cured composite was studied under both quasi-static and dynamic modes. Our studies revealed that the shell wall of the microcapsule did not play any significant role in defining the mechanical properties of the resulting composite, which was found to decrease proportionally with increasing loading. Significant improvement in the toughness of the base resin was observed, which was attributed to underlying mechanisms like crack pinning, crack bowing, microcracking and crack path deflection as evidenced by fractographic investigations.

## EXPERIMENTAL

### Materials

Epoxy monomer, (Araldite CY 230; epoxy equivalent 200 eq/g) as well as triethylene tetramine (TETA) based curing agent (HY 951; amine content 32 eq/kg) was purchased from Ciba Geigy, and used as received. Urea, melamine, formalin (37% formaldehyde in water), citric acid, polyvinyl alcohol (PVA) ( $M_w = 14,000$ ) was obtained from CDH. Triethanolamine (Merck) was used without any further purification. Distilled water was used throughout the course of this work.

### Preparation of Microcapsules

Epoxy encapsulated microcapsules were prepared by an in situ oil-in-water (O/W) emulsion polymerization route using the

procedure reported in the literature with slight modifications.<sup>14</sup> Urea (5 g) and formalin (10 g) was dissolved in distilled water (35 mL) under continuous stirring at room temperature. The pH of resulting solution was subsequently increased to 8–9 by dropwise addition of triethanolamine, while maintaining the temperature at  $70 \pm 5^\circ\text{C}$  for 1 h to obtain a prepolymer solution. This was cooled to room temperature and an aqueous solution of PVA (2.5 mL, 5% w/w) was introduced, which was followed by the addition of a slow stream of epoxy resin to form an emulsion. Post stabilization, the pH was slowly brought down to 3–4 by addition of an aqueous citric acid solution (1 mL, 5% w/v) while increasing the temperature of the solution at a rate of  $1^\circ\text{C min}^{-1}$  to the target temperature of  $50 \pm 3^\circ\text{C}$ . After 3 h, the obtained suspension of microcapsules was cooled, filtered, washed repeatedly with distilled water and acetone, and air-dried for 24 h. Epoxy encapsulated melamine-formaldehyde (MF) microcapsules were also prepared in a similar manner, while using melamine instead of urea, all other reaction parameters remaining same. A schematic showing the reaction of the amino groups in melamine and urea with methanal is presented in the supplementary section (Supporting Information Schemes S1 and S2).

The extent of encapsulation in the microcapsules was determined by acetone extraction method as per the reported procedure.<sup>7</sup> For this purpose, an accurately weighed amount of microcapsules ( $M_{mc}$ ) was crushed to release the encapsulated healing agent. The resulting powder was then washed with acetone, filtered, dried, and weighed ( $M_{shell}$ ). The core content was determined gravimetrically as the ratio of encapsulated mass of epoxy ( $M_{mc} - M_{shell}$ ) to the initial mass of the microcapsules ( $M_{mc}$ ).

### Preparation of Epoxy Composites

Epoxy composites containing varying amounts of either UF or MF microcapsules (5–15% w/w) were prepared by room temperature curing of epoxy with TETA hardener. For this purpose, the epoxy encapsulated microcapsules were first sieved through a 40–100 mesh (BSS), to obtain microcapsules of desired particle dimensions (150–425  $\mu\text{m}$ ), which were subsequently dispersed in the epoxy resin and ultrasonicated to aid homogenization. Requisite amount of TETA hardener was added, and the suspension was degassed under vacuum and transferred to greased silicone moulds, where the curing reaction was allowed to proceed at  $30^\circ\text{C}$  for 24 h. Neat epoxy specimens were also prepared in a similar manner, which will be referred to as EP in the subsequent text. The details of all the compositions prepared along with their sample designations are presented in Table I. All the cured epoxy formulations containing microcapsules will be referred to as EPxZ where x refers to the amount of loading (% w/w) and Z refers to type of microcapsules (UF or MF) used for its preparation. For example, EP5UF refers to a cured epoxy composition containing UF microcapsules (5% w/w).

### Characterization

FTIR spectra of samples were recorded in the wavelength range  $4000\text{--}600\text{ cm}^{-1}$  using a Thermo Fisher FTIR (NICOLET 8700) analyzer with an attenuated total reflectance (ATR) crystal

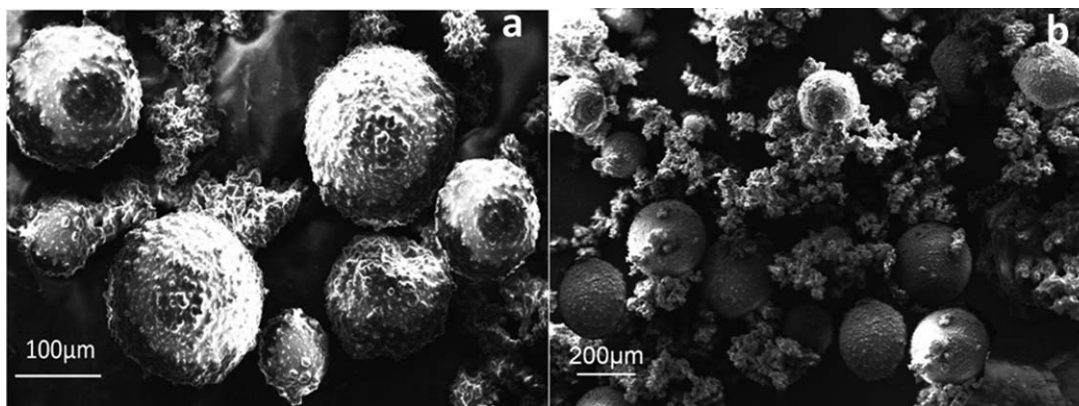


**Figure 1.** SEM image of epoxy encapsulated microcapsules (a) Urea-formaldehyde (b) Melamine-formaldehyde.

accessory. Calorimetric studies were performed on a Differential Scanning Calorimeter (TA instruments Auto Q 20). The epoxy resin and curing agent (TETA) were mixed at a stoichiometric epoxide/TETA ratio (100 : 13) at low temperatures (0–5°C). For dynamic DSC scans, samples ( $10 \pm 2$  mg) were sealed in aluminum pans, and heated from 273 K to 523 K at 5°C/min under nitrogen atmosphere to minimize sample oxidation during curing. Prior to the experiments, the instrument was calibrated for temperature and enthalpy using standard indium and zinc. Thermal equilibrium was regained within 1 min of sample

insertion, and the exothermic reaction was considered to be complete when the recorder signal leveled off to the baseline. The total area under the exothermic curve was determined to quantify the heat of curing. The thermal behavior was investigated using Perkin Elmer Diamond STG-DTA under  $N_2$  atmosphere in the temperature range 50–800°C. A heating rate of 10°C/min and sample mass of  $5.0 \pm 0.5$  mg was used for each experiment. The quasi-static mechanical properties, were determined as per ASTM method D638 using a Universal Testing System (International equipments) at ambient temperature. The

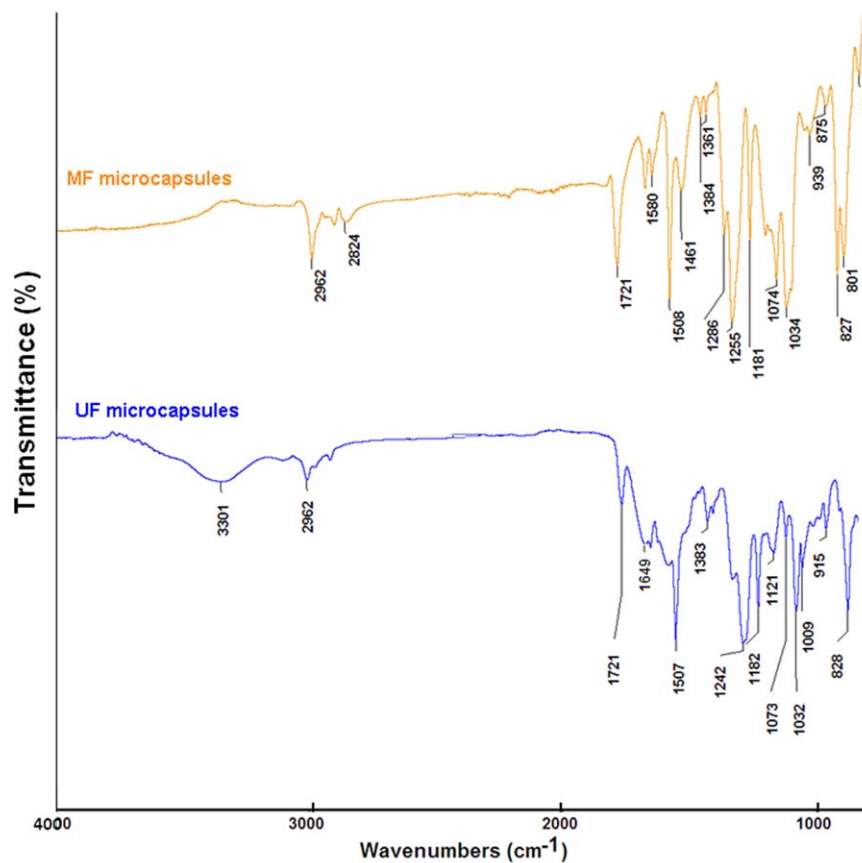


**Figure 2.** FTIR spectra of epoxy encapsulated UF and MF microcapsules. [Color figure can be viewed in the online issue, which is available at wileyonlinelibrary.com.]

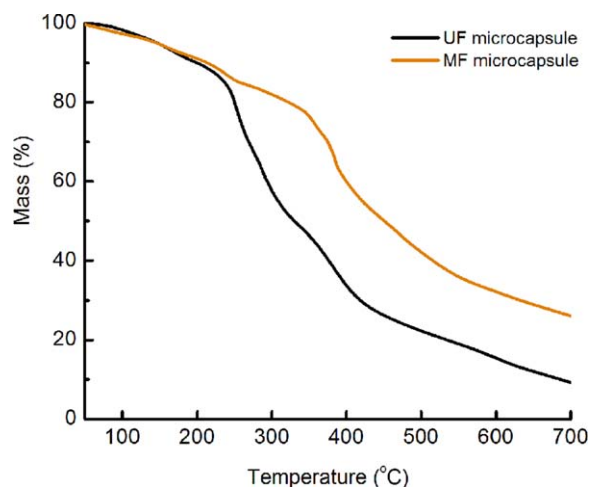


**Figure 3.** TG traces of epoxy encapsulated urea-formaldehyde and melamine-formaldehyde microcapsules. [Color figure can be viewed in the online issue, which is available at [wileyonlinelibrary.com](http://wileyonlinelibrary.com).]

dog-bone shaped specimens used for tensile testing were 165-mm long, 3-mm thick, and 13-mm wide along the centre of the casting for epoxy resin. The samples were subjected to a cross head speed of  $50 \text{ mm min}^{-1}$ . The notched Izod impact strength of the specimens was determined as per ASTM D 256 using an impact strength testing machine (International Equipments, India). Flexural testing of the samples was performed under three point single edge notch bending mode using the same instrument. For this purpose, specimens with requisite dimensions ( $127\text{-mm length} \times 12.5\text{-mm width} \times 3.5\text{-mm thickness}$  and 3-mm notch) were prepared and the samples were subjected to a deformation rate of  $2 \text{ mm min}^{-1}$  while maintaining a span length of 60 mm. The mode I critical stress intensity factor ( $K_{IC}$ ) of the samples was determined as per the following equation<sup>15</sup>:

$$K_{IC} = \frac{3 \times P \times L \times a^{1/2}}{2 \times B \times w^2} Y \left( \frac{a}{w} \right) \quad (1)$$

where  $P$ ,  $L$ , and  $B$  refer to the load at break, span length, and sample thickness, respectively. The geometry factor,  $Y \left( \frac{a}{w} \right)$  is calculated as per the formula below, where “ $a$ ” is the notch length and “ $w$ ” is the sample width.

$$Y \left( \frac{a}{w} \right) = 1.93 - 3.07 \times \left( \frac{a}{w} \right) + 14.53 \times \left( \frac{a}{w} \right)^2 - 25.11 \times \left( \frac{a}{w} \right)^3 + 25.8 \times \left( \frac{a}{w} \right)^4 \quad (2)$$

The  $K_{IC}$  was used to estimate the fracture energy ( $G_{IC}$ ), which was calculated using the following equation

$$G_{IC} = \frac{K_{IC}^2 (1 - \nu^2)}{E} \quad (3)$$

where  $E$  is the flexural modulus of the polymer, and  $\nu$  is the Poisson's ratio of epoxy (0.35).<sup>16</sup> For each composition, at least five identical specimens were tested and the average results along with the standard deviation have been reported. The surface morphology of samples was studied using a Scanning Electron Microscope (Zeiss EVO MA15) under an acceleration voltage of 20 kV. Samples were mounted on aluminium stubs and sputter-coated with gold and palladium

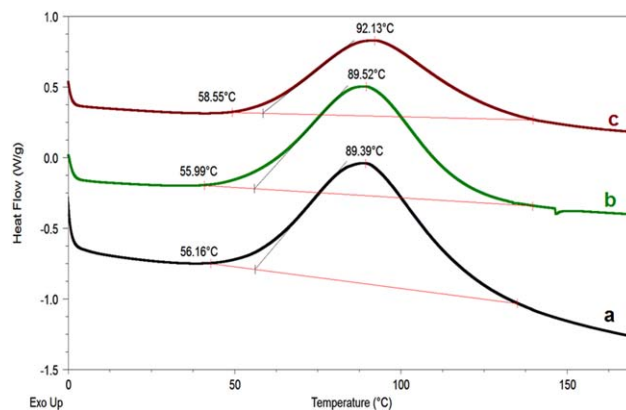


**Figure 4.** Curing profile of epoxy based compositions (a) Neat epoxy, (b) EP10UF, (c) EP10MF. [Color figure can be viewed in the online issue, which is available at [wileyonlinelibrary.com](http://wileyonlinelibrary.com).]

(10 nm) using a sputter coater (Quorum-SC7620) operating at 10–12 mA for 120 s.

## RESULTS AND DISCUSSION

### Characterization of Epoxy Encapsulated Microcapsules

The morphology of a representative batch of epoxy encapsulated UF and melamine-formaldehyde microcapsules is presented in Figure 1. It can be seen that the microcapsules are spherical in shape, and exhibit a rough surface texture, a feature which could be attributed to the presence of protruding polymer nanoparticles.<sup>13</sup> The interior of the microcapsule is however smooth and the thickness of the shell wall, as determined from the SEM images was found to be  $\sim 350 \pm 54 \text{ nm}$  (Supporting Information Figure S1). The microcapsule size could be controlled by varying the rate of agitation during the polymerization process. However, for this study, a stirring speed of 250 rpm was employed, which yielded microspheres of dimensions satisfactory for the use in self-healing application,<sup>13</sup> i.e., (diameter  $\sim 190 \pm 49 \mu\text{m}$  for UF microcapsules and  $219 \pm 35 \mu\text{m}$  for MF microcapsules). The core content of the microcapsules was

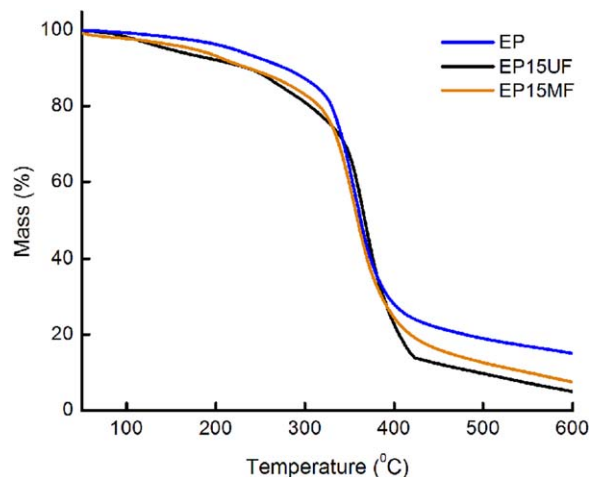


**Figure 5.** TG traces of composites formed with microcapsules. [Color figure can be viewed in the online issue, which is available at [wileyonlinelibrary.com](http://wileyonlinelibrary.com).]



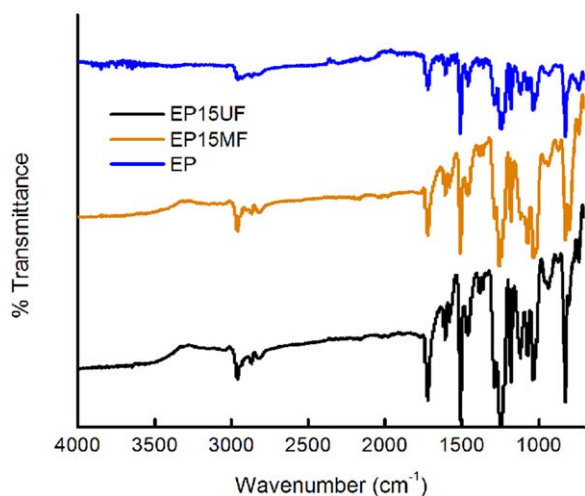


**Figure 6.** FTIR spectra of composites. [Color figure can be viewed in the online issue, which is available at [wileyonlinelibrary.com](http://wileyonlinelibrary.com).]

determined to be  $65 \pm 5\%$  irrespective of the polymer used for encapsulation.

FTIR spectra of MF and UF microcapsules are presented in Figure 2. MF microcapsules exhibit characteristic broad band around  $3350 \text{ cm}^{-1}$  which arises from the overlapping absorptions due to hydroxyl, imino and amino functionalities. Other characteristic absorptions include alkyl C—H stretching ( $2962 \text{ cm}^{-1}$ ), C—H bending ( $1461 \text{ cm}^{-1}$  and  $1361 \text{ cm}^{-1}$ ), aliphatic C—N ( $1255$  and  $1181 \text{ cm}^{-1}$ ), triazine ring ( $1580 \text{ cm}^{-1}$ ) and C—O—C stretching ( $1034 \text{ cm}^{-1}$ ). The UF microcapsules also exhibit absorption bands in the same region, besides additional absorption at  $1649 \text{ cm}^{-1}$  due to NH—CO—NH stretching.<sup>17</sup>

The TG traces of epoxy encapsulated UF and MF microcapsules are presented in Figure 3. The thermal degradation of MF reportedly occurs in stepwise fashion.<sup>18</sup> The initial mass loss of  $\sim 3.6\%$  ( $T < 150^\circ\text{C}$ ) can be attributed to the removal of water, and the subsequent loss of  $11.2\%$  ( $145\text{--}245^\circ\text{C}$ ) occurs due to the removal of methanol and formaldehyde formed as a result

of thermal decomposition. At  $T > 400^\circ\text{C}$ , pyrolytic degradation of the three-dimensional framework reportedly occur leading to the evolution of ammonia and formaldehyde.<sup>17</sup> In comparison, the UF microcapsules exhibit lower thermal stability. The transformation of methylene ether bridges into methylene bridges occurs at  $\sim 200^\circ\text{C}$ , which is associated with loss of formaldehyde and the subsequent mass loss at  $300\text{--}390^\circ\text{C}$  occurs due to pyrolytic degradation of the crosslinked network. Microcapsules with MF in the shell wall exhibit significantly higher char content ( $26\%$  at  $700^\circ\text{C}$ ) than UF ( $9\%$  at  $700^\circ\text{C}$ ), which can be attributed to the presence of thermally stable cyameluric structures in the former.

### Epoxy-Microcapsule Composites

Epoxy composites were prepared by dispersing requisite amounts of either MF or UF microcapsules in epoxy resin by ultrasonication, followed by curing under ambient conditions. The DSC traces of neat epoxy and microcapsule filled compositions under a programmed heating rate ( $5^\circ\text{C}/\text{min}$ ) are presented in Figure 4. It is apparent from the figure that all the compositions exhibit a single peak, which is characteristic of the exothermic nature of the curing process. Interestingly, the presence of UF or MF microcapsules did not affect the curing process appreciably and all the compositions exhibit similar onset cure temperature ( $T_{\text{onset}}$ ) and peak cure temperature ( $T_{\text{peak}}$ ) values. The TG trace of cured epoxy and its composites with different microcapsules is presented in Figure 5. It can be seen that the introduction of epoxy encapsulated microcapsules lead to a slight reduction in the thermal stability of the base polymer. Temperature corresponding to  $5\%$  mass loss ( $T_{5\%}$ ) of epoxy ( $220^\circ\text{C}$ ) is lowered to  $175^\circ\text{C}$  and  $147^\circ\text{C}$  due to introduction of MF and UF microcapsules ( $15\%$  w/w), respectively. Also, in comparison with neat epoxy, the char content of the microcapsule loaded samples is slightly lower, which can be attributed to the presence of uncured resin within the microcapsules.

The FTIR spectrum of cured epoxy and composites prepared in the presence of microcapsules is presented in Figure 6. As expected an increased absorption in the region above  $3300$

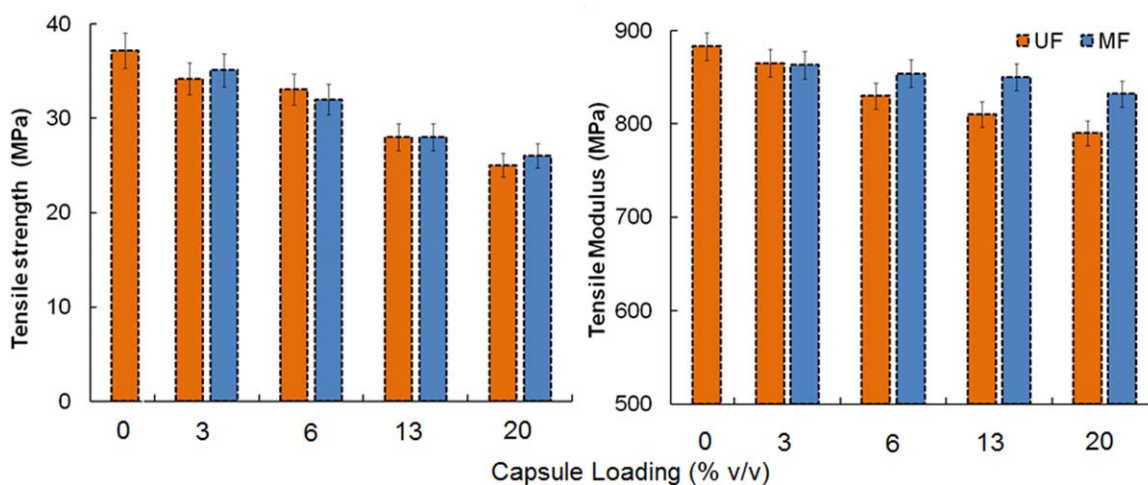


**Figure 7.** Effect of inclusion of UF and MF on the tensile strength and modulus of epoxy. [Color figure can be viewed in the online issue, which is available at [wileyonlinelibrary.com](http://wileyonlinelibrary.com).]

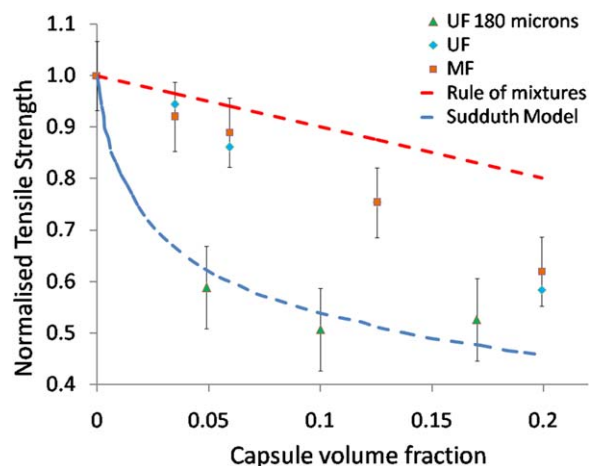


**Figure 8.** Normalised tensile strength of epoxy-microcapsule composite compared with “Sudduth model” and “rule of mixtures.” Previously reported data<sup>21</sup> of 180  $\mu\text{m}$  UF microcapsules also presented for purpose of comparison. [Color figure can be viewed in the online issue, which is available at [wileyonlinelibrary.com](http://wileyonlinelibrary.com).]

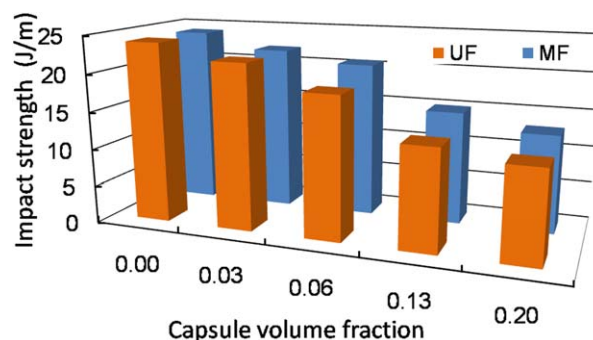
$\text{cm}^{-1}$  is observed in the composites, which could be attributed to the absorption due to hydroxyl, imino and amino groups present in the shell wall of the microcapsules.

Figure 7 presents the variation in mechanical properties of the epoxy as a function of volume fraction of UF and MF microcapsules. For estimation of the volume fraction, the density of microcapsules ( $\rho_{\text{mc}}$ ) and epoxy ( $\rho_{\text{epoxy}}$ ) was assumed to be  $1000 \text{ kg m}^{-3}$  and  $1160 \text{ kg m}^{-3}$ , respectively.<sup>19</sup> It can be seen that the introduction of microcapsules resulted in a reduction in both the tensile strength and modulus, the extent of which was found to be proportional to the amount of microcapsule loading. Previous studies have revealed that MF microcapsules are mechanically much stronger than UF,<sup>10,11</sup> but due to the fragile nature, their contribution to the load bearing capability of epoxy seems to be practically negligible, which can be used to explain the observed reduction in the mechanical properties of the resultant composites. Our results clearly indicate that the shell wall of the microcapsule does not play any significant role in defining the mechanical properties, which were found to depend only on the extent of loading.

Our results were compared with reported results of previous investigations<sup>12</sup> and empirical models proposed by Sudduth for particulate fillers.<sup>20</sup> For comparison purposes, a plot of  $\sigma_c/\sigma_o$  with volume fraction, as expected on the basis of rule of mixtures is also presented in Figure 8. As per Sudduth, the normalized tensile strength can be modeled as follows:

$$\frac{\sigma_c}{\sigma_o} = \left( \frac{\phi_{\text{FZL}} - \phi_f}{\phi_{\text{FZL}} + A\phi_f} \right)^\lambda \exp \left[ B\phi_{\text{FZL}} \left\{ 1 - \left( \frac{\phi_{\text{FZL}} - \phi_f}{\phi_{\text{FZL}} + A\phi_f} \right)^\lambda \right\} \right]$$

where  $\sigma_c$  and  $\sigma_o$  are the tensile strength of composite sample and neat resin. The interaction coefficient ( $\lambda$ ),  $A$  and  $B$  are fitting parameters and  $\phi_{\text{FZL}}$  is the zero limit packing fraction which has been assumed to be the upper zero limit packing fraction (0.768).<sup>20</sup> It can be seen that our data lies within the values predicted on the basis of Sudduth model and rule of



**Figure 9.** Decrease in impact strength of epoxy due to inclusion of UF and MF microcapsules. [Color figure can be viewed in the online issue, which is available at [wileyonlinelibrary.com](http://wileyonlinelibrary.com).]

mixtures, which clearly highlight the important role of adhesion between the microcapsules and base epoxy resin in defining the mechanical properties.

The introduction of microcapsules also led to a proportional decrease in the impact strength of epoxy, as is evident from data presented in Figure 9. The impact strength decreased from  $24 \pm 1.5 \text{ J m}^{-1}$  (neat resin) to  $12 \pm 1 \text{ J m}^{-1}$  after addition of 15% w/w microcapsules irrespective of the shell wall material. Similar extent of impact strength lowering has been reported previously on epoxy samples containing healant encapsulated UF microcapsules.<sup>21</sup>

The flexural stress-strain response of the compositions prepared is presented in Figure 10. Interestingly, the composites exhibited higher strength and modulus in comparison with the unmodified epoxy. The mechanical response of notched specimens is also presented in Figure 10 (Inset), which clearly elicit the detrimental effect of notch on the flexural strength, which in turn can be attributed to stress concentration resulting from the smaller cross-sectional area.

Single edge notch bend (SENB) geometry is the most common mode for quantification of fracture toughness of polymeric

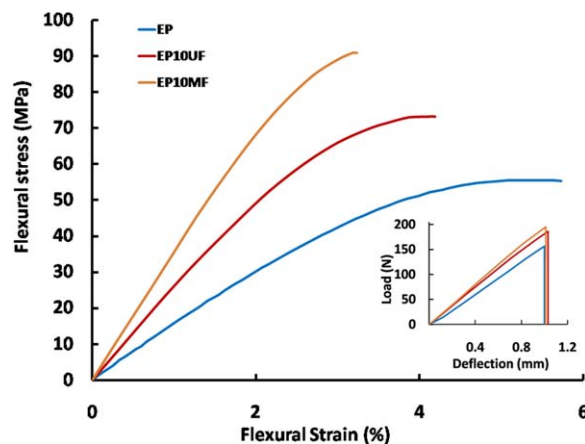


**Figure 10.** Representative stress-strain curves of epoxy and its composites with UF and MF microcapsules (flexural mode). Inset shows the effect of notch on the flexural response of specimens. [Color figure can be viewed in the online issue, which is available at [wileyonlinelibrary.com](http://wileyonlinelibrary.com).]

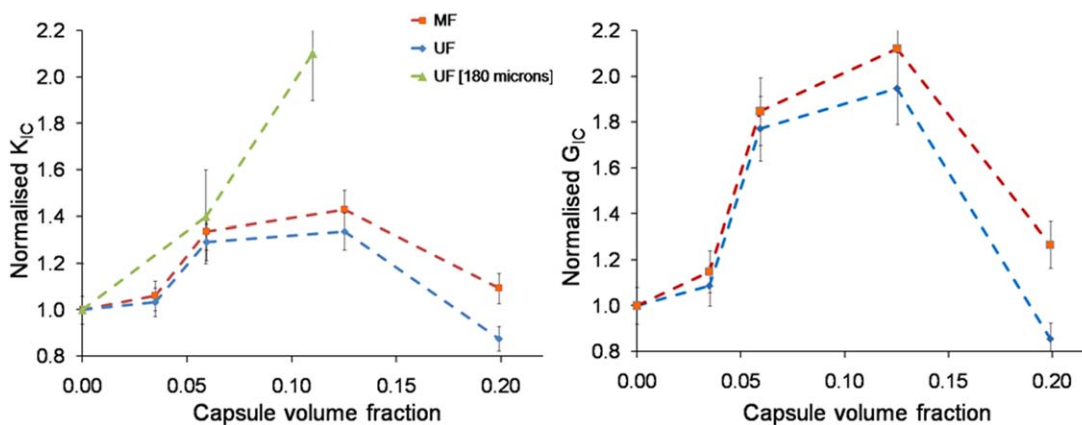


**Figure 11.** Increase in the normalized critical stress intensity factor ( $K_{IC}$ ) and normalized fracture energy ( $G_{IC}$ ) due to inclusion of microcapsules. Results of previous study (180  $\mu\text{m}$  UF capsules)<sup>21</sup> is also presented. [Color figure can be viewed in the online issue, which is available at wileyonlinelibrary.com.]

samples,<sup>15</sup> however, for self-healing compositions, the use of tapered double-cantilever beam (TDCB) geometry has also been used.<sup>22</sup> In this study, we have determined the toughness, using the SENB geometry in order to allow comparison with our previous studies.<sup>23,24</sup>

A comparison of normalized critical stress intensity factor ( $K_{IC}$ ) and fracture energy ( $G_{IC}$ ) as a function of microcapsule loading is presented in Figure 11. The actual values of  $K_{IC}$  and  $G_{IC}$  are presented in the supplementary section (Supporting Information Figure S2). For the purpose of calculation, the Poisson's ratio of epoxy was assumed to be 0.35.<sup>16</sup> It is apparent from the figure that the stress intensity factor  $K_{IC}$  of epoxy increased by  $\sim 38.2 \pm 6\%$  on the introduction of microcapsules (10% w/w), irrespective of the shell wall material used for encapsulation of liquid healant. This is however much lesser than the value of 127% reported previously, an incongruity which may be attributed to the TCDB geometry used for toughness determination<sup>25</sup> as compared with SENB geometry used in this work.  $K_{IC}$  was further used to calculate the fracture energy, which was found to increase substantially, from a mean value of  $5.05 \text{ kJ/m}^2$  (unmodified epoxy) to  $9.5 \pm 0.4 \text{ kJ/m}^2$  after loading of microcapsules (10% w/w) irrespective of shell wall material.

It was interesting to note the difference in the fracture toughness values estimated from impact and single edge notched bending tests. Comparison of Figures 9 and 11 reveals that the

ized impact toughness decreases, while the SENB fracture toughness increase with microcapsule addition. This may be attributed to the difference in the strain rate employed, with the latter being performed at much lower strain rates ( $8.1 \times 10^{-2} \text{ s}^{-1}$ ) giving the polymer enough time to respond to the applied stress.

#### Toughening Mechanism

Fractography was performed on the cracked surfaces, and the results are presented in Figures 12 and 13. The smooth and featureless surface of epoxy is characteristic of fracture in a brittle thermosetting polymer, which exhibits no signs of plastic deformation (Figure 12).<sup>26,27</sup> The presence of feather-like hackle markings resulting from small-scale secondary crack formation could be observed just after the plastic zone which extends to the stress zone. The hackle markings transition into striations in the direction of crack propagation and finally there is a complete transition to a mirror fracture surface, as reported previously.<sup>25</sup>

In comparison, the fractured surface of the epoxy containing microcapsules is rather rough throughout the crack plane. Toughening by "crack pinning" is most commonly cited to explain the toughened nature of filled epoxy. According to this, the role of second phase is to cause the crack front to bow out, propagation of which requires much larger amount of energy. Indirect evidence of the occurrence of this mechanism is the

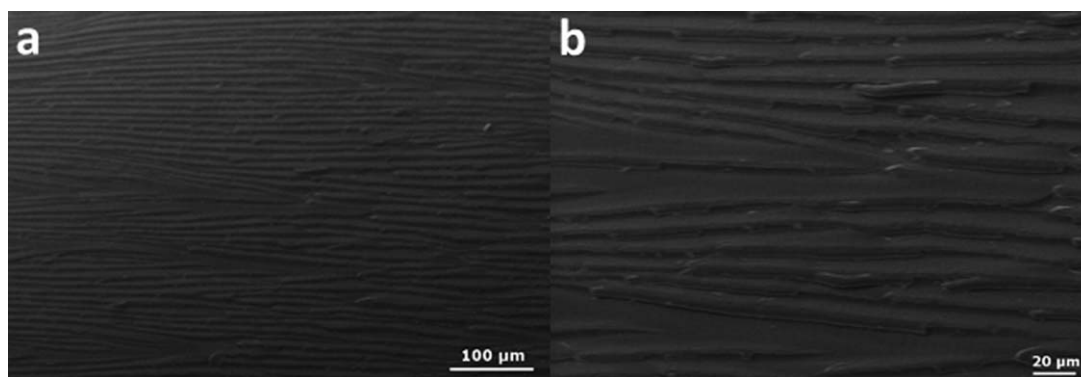


**Figure 12.** SEM image of fractured epoxy at different magnifications.



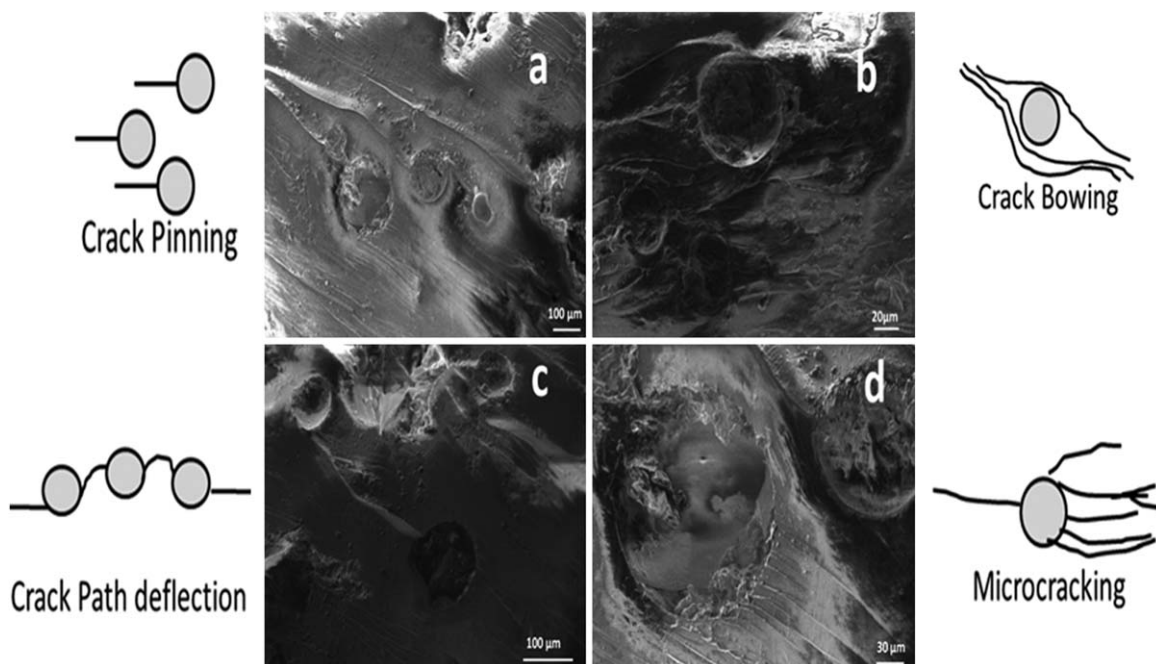


**Figure 13.** Pictorial schematic of the underlying toughening mechanisms along with SEM images of fracture surface revealing (a) crack pinning, (b) crack bowing, (c) crack path deflection, (d) microcracking.

presence of “tails” associated with the embedded microcapsules [Figure 13(a)]. In certain cases, the crack front is forced to change its path as it approaches the microcapsules, a phenomenon more commonly known as crack bowing, [Figure 13(b)], which results in increased surface area. Further, the mode I character of the crack opening is also reduced, which in turn requires larger amount of energy for its propagation.

As expected, a number of “broken” microcapsules were observed on the surface of the composite. It appears that the “breaking” of the microcapsule leads to the flow of the encapsulated healant into the crack plane. In rigid particle-epoxy composites,<sup>28</sup> crack pinning by the filler material is expected to contribute significantly towards increasing the toughness of the composite. However, in the present scenario, due to the fragile nature of the microcapsules, the contribution of this route is practically negligible. However, clear evidence of “Crack path deflection” [Figure 13(c)] and “Microcracking” [Figure 13(d)] was found during fractography,<sup>29</sup> which could be used to explain the toughened nature of the microcapsule containing composite samples.

## CONCLUSION

Liquid epoxy resin was encapsulated in UF and MF microcapsules using emulsion polymerization technique. The effect of inclusion of microcapsules on the thermal, structural and mechanical properties of a representative cycloaliphatic thermo-setting epoxy resin was studied under both quasi-static and dynamic loadings. Interestingly, the shell wall of the microcapsule was found to play an insignificant role in defining the

mechanical properties of the resulting composite, which was found to decrease proportionally with microcapsule loading. However, significant improvement in the toughness of the base resin was achieved ( $38.2 \pm 6\%$ ), which was quantified in terms of critical stress intensity factor ( $K_{IC}$ ) and fracture energies ( $G_{IC}$ ). Fractography of the cracked surface was performed to gain insight into the underlying mechanisms behind the improved toughening. Clear evidence of crack pinning, crack bowing, microcracking and crack path deflection was observed during morphological investigations, which could be used to explain the toughened nature of the composites. The presence of UF or MF microcapsules did not affect the curing behavior of epoxy and all the compositions were found to exhibit similar onset and peak cure temperatures.

## ACKNOWLEDGMENTS

The authors are thankful to Director, Centre for Fire, Explosive and Environment Safety, Delhi, India for his keen interest in the work and providing logistic support to perform the study.

## REFERENCES

1. Yuan, Y. C.; Yin, T.; Rong, M. Z.; Zhang, M. Q. *Exp. Polym. Lett.* **2008**, *2*, 238.
2. Wu, D. Y.; Meure, S.; Solomon, D. *Prog. Polym. Sci.* **2008**, *33*, 479.
3. Kessler, M. R.; Sottos, N. R.; White, S. R. *Compos. Part A: Appl. Sci. Manuf.* **2003**, *34*, 743.



4. Brown, E. N.; White, S. R.; Sottos, N. R. *Compos. Sci. Technol.* **2005**, *65*, 2466.
5. Brown, E. N.; White, S. R.; Sottos, N. R. *Compos. Sci. Technol.* **2005**, *65*, 2474.
6. Blaiszik, B. J. *Polymer* **2009**, *50*, 990.
7. Yuan, L.; Liang, G.; Xie, J.; Li, L.; Guo, J. *Polymer* **2006**, *47*, 5338.
8. White, S. R.; Sottos, N. R.; Geubelle, P. H.; Moore, J. S.; Kessler, M. R.; Sriram, S. R.; Brown, E. N.; Viswanathan, S. *Nature* **2001**, *409*, 794.
9. Zhang, Z.; Saunders, R.; Thomas, C. R. *J. Microencapsulation* **1999**, *16*, 117.
10. Keller, M. W.; Sottos, N. R. *Exp. Mech.* **2006**, *46*, 725.
11. Sun, G.; Zhang, Z. *Int. J. Pharm.* **2002**, *242*, 307.
12. Blaiszik, B. J.; Sottos, N. R.; White, S. R. *Compos. Sci. Technol.* **2008**, *68*, 978.
13. Brown, E. N. *J. Microencapsulation* **2003**, *20*, 719.
14. Yuan, Y. C.; Rong, M. Z.; Zhang, M. Q.; Chen, J.; Yang, G. C.; Li, X. M. *Macromolecules* **2008**, *41*, 5197.
15. Knott, J. F., *Fundamentals of Fracture Mechanics*; Butterworths; London, **1976**.
16. Kinloch, A. J., *Adhesion and Adhesives: Science and Technology*; Chapman & Hall: London, **1987**.
17. Salaün, F.; Vroman, I. *Eur. Polym. J.* **2008**, *44*, 849.
18. Zorba, T.; Papadopoulou, E.; Hatjiissaak, A.; Paraskevopoulos, K. M.; Chrissafis, K. *J. Therm. Anal. Calorim.* **2008**, *92*, 29.
19. Brown, E. N.; White, S. R.; Sottos, N. R. *J. Mater. Sci.* **2006**, *41*, 6266.
20. Sudduth, R. D. *J. Compos. Mater.* **2006**, *40*, 301.
21. Xiao, D. S.; Yuan, Y. C.; Rong, M. Z.; Zhang, M. Q. *Polymer* **2009**, *50*, 2967.
22. Brown, E. N.; Sottos, N. R.; White, S. R. *Exp. Mech.* **2002**, *42*, 372.
23. Chaudhary, S.; Parthasarathy, S.; Kumar, D.; Rajagopal, C.; Roy, P. K. *J. Appl. Polym. Sci.* **2014**, *131*.
24. Roy, P.; Iqbal, N.; Kumar, D.; Rajagopal, C. *J. Polym. Res.* **2014**, *21*, 1.
25. Brown, E. N.; White, S. R.; Sottos, N. R. *J. Mater. Sci.* **2004**, *39*, 1703.
26. Williams, J. G. *Compos. Sci. Technol.* **2010**, *70*, 885.
27. Voo, R.; Mariatti, M.; Sim, L. C. *Compos. Part B: Eng.* **2012**, *43*, 3037.
28. Roy, P. K.; Ullas, A. V.; Chaudhary, S.; Mangla, V.; Sharma, P.; Kumar, D.; Rajagopal, C. *Iran. Polym. J.* **2013**, *22*, 709.
29. Pearson, R. A.; Yee, A. F. *Polymer* **1993**, *34*, 3658.